Mechanism of *Salmonella typhimurium* Histidinol Dehydrogenase: Kinetic Isotope Effects and pH Profiles†

Charles Grubmeyer* and Henry Teng‡

Department of Biochemistry and Fels Institute for Cancer and Molecular Biology, Temple University School of Medicine, 3307 North Broad Street, Philadelphia, Pennsylvania 19140

Received November 19, 1998; Revised Manuscript Received March 16, 1999

ABSTRACT: L-Histidinol dehydrogenase catalyzes the biosynthetic oxidation of L-histidinol to L-histidine with sequential reduction of two molecules of NAD. Previous isotope exchange results had suggested that the oxidation of histidinol to the intermediate histidinaldehyde occurred 2−3-fold more rapidly than overall catalysis. In this work, we present kinetic isotope effects (KIE) studies at pH 9.0 and at pH 6.7 with stereospecifically mono- and dideuterated histidinols. The data at pH 9.0 support minimal participation of the first hydride transfer and substantial participation of the second hydride transfer in the overall rate limitation. Stopped-flow experiments with protiated histidinol revealed a small burst of NADH production with stoichiometry of 0.12 per subunit, and 0.25 per subunit with dideuterated histidinol, indicating that the overall first half-reaction was not significantly faster than the second reaction sequence. Results from k_{cat} and k_{cat}/K_M titrations with histidinol, NAD, and the alternative substrate imidazolyl propanediol demonstrated an essential base with pK_a values between 7.7 and 8.4. In KIE experiments performed at pH 6.7 or with a coenzyme analogue at pH 9.0, the first hydride transfer became more rate limiting. Kinetic simulations based on rate constants estimated from this work fit well with a mechanism that includes a relatively fast, and thermodynamically unfavorable, hydride transfer from histidinol and a slower, irreversible second hydride transfer from a histidinaldehyde derivative. Thus, although the chemistry of the first hydride transfer is fast, both partial reactions participate in the overall rate limitation.

L-Histidinol dehydrogenase (HDH,[1] EC 1.1.1.23) is an NAD-linked four-electron dehydrogenase that catalyzes the final step in the biosynthesis of histidine. The enzyme is of interest because its single active site carries out oxidations of both the histidinol substrate and an aldehyde-level intermediate, sequentially reducing two NAD molecules (*1*−*3*). Both reductions proceed via R stereochemistry at NAD (*4*−*6*) and during the oxidative reactions remove first the *pro-S* and then the *pro-R* hydroxymethyl hydrogen of histidinol (*5*). The energetic and chemical problems implicit in the catalysis of two distinct reactions at a single site may have general significance for dehydrogenase mechanism.

The most puzzling feature of the HDH reaction is the aldehyde-oxidizing half-reaction. Adams (*1*) observed that the presence of aldehyde-derivitizing reagents did not affect overall catalysis by HDH and suggested that histidinal, the proposed intermediate, did not dissociate from the active site during overall catalysis. Görisch and Hölke (*7*) verified that externally added histidinal was bound very tightly to HDH (see also ref *8*) and was protected from alkaline degradation. These results led to the hypothesis that enzyme-bound histidinal exists as an adduct with an enzymic nucleophile. Imine and thiohemiacetal chemistries of the adduct (*9*, *10*) have been ruled out (*11*−*13*). A tightly bound hydrated histidinal (*gem*-diol) is an alternative intermediate (*13*). Hydrated aldehydes have been proposed for glyoxylate oxidation by pig heart L-lactate dehydrogenase (*14*), the oxidation of glyceraldehyde-3-phosphate by a mutant form of glyceraldehyde-3-phosphate dehydrogenase (*15*), as substrates for *Drosophila* ADH (*16*), and during the oxidations of acetaldehyde and benzaldehyde by horse liver ADH (*17*, *18*).

The steady-state mechanism of the HDH reaction has been investigated by Görisch (*19*) and Bürger and Görisch (*20*), who showed that HDH was kinetically bi-uni-uni-bi ping-pong, with histidinol the leading substrate. We have used binding studies and exchange reactions to confirm that unliganded *Salmonella* HDH can bind histidinol, and that NAD binds second in apparent compulsory order (*21*). Recent steady-state studies with the *Brassica* HDH showed an identical kinetic scheme (*8*). The ordered binding of substrate before coenzyme is unusual among dehydrogenases, being shared by uridine diphospho-α-D-glucose dehydrogenase, another NAD-linked four-electron dehydrogenase (*22*, *23*), yeast aldehyde dehydrogenase (*24*), and inosine 5-monophosphate dehydrogenase (*25*).

† This work was supported by the National Institute of Health.

* To whom correspondence should be addressed. Phone: 215-707-4495, FAX: 215-707-5529, e-mail: ctg@ariel.fels.temple.edu.

‡ Current address: Department of Microbiology, University of Pennsylvania School of Medicine, 3610 Hamilton Walk, Philadelphia, PA 19104.

[1] Abbreviations: AcPAD, oxidized or reduced 3-acetylpyridine adenine dinucleotide; ADH, alcohol dehydrogenase; HDH, L-histidinol dehydrogenase; Hepes, *N*-(2-hydroxyethyl)piperazine-*N*′-(2-ethanesulfonic acid); histidinal, L-histidinaldehyde; KIE, kinetic isotope effects; SDS−PAGE, sodium dodecyl sulfate−polyacrylamide gel electrophoresis.

10.1021/bi982757x CCC: $18.00
Published on Web 05/13/1999

Isotope-exchange studies with HDH indicated that the histidinol oxidation (first half-reaction) was at least 2−3-fold faster than overall k_{cat}, suggesting that the overall rate limitation lies within the histidinal oxidation [second half-reaction (*21*)]. In the current work, kinetic isotope effects, isotope trapping, pH profiles, and stopped-flow spectrophotometry are used to study the two half-reactions. A kinetic mechanism is developed with a fast reversible oxidation of histidinol, followed by the slow irreversible hydride transfer from histidinal. Kinetic simulations based on this mechanism provide a good fit to experimentally obtained data.

MATERIALS AND METHODS

Materials. L-Histidinol, L-histidine methyl ester, imidazolyl lactic acid, and other biochemicals were obtained from Sigma. [^{14}C]Histidine labeled at C-2 of the imidazole ring was from DuPont NEN and Sigma. NAD (free acid, grade I) was from Boehringer. Hepes was from Research Organics. Thin-layer chromatography plates of cellulose (0.1 mm Macherey Nagel) were obtained from Brinkmann. DEAE-cellulose (DE−52) was from Whatman. Dowex resin was from Aldrich. Enzymatic and chemical syntheses of diprotiated and dideuterated imidazolyl propanediols and various forms of deuterated, tritiated, and [^{14}C]histidinol (from [^{14}C]-histidine) were carried out as described (*5*, *21*) using chemical and enzymatic procedures. When substrate deuterium kinetic isotope effects were being determined, unsubstituted substrates were synthesized by the same procedures (enzymatic for histidinol, chemical for imidazolyl propanediol) as the deuterated compounds, to obviate the effects of inhibitors that might arise during the syntheses. Isotopic incorporation in deuterated histidinol was assessed by NMR according to Grubmeyer et al. (*5*). In referring to deuterium- and tritium-labeled histidinol, the order of letters corresponds to the order of hydride removal in the overall HDH reaction. Thus, with (D,H)histidinol {[hydroxymethyl-(*S*)-^{2}H]histidinol} and (H,D)-histidinol {[hydroxymethyl-(*R*)-^{2}H]histidinol}, the deuterides are transferred during the first and second half-reactions respectively, whereas with (D,D)histidinol, deuterides are transferred during both half-reactions.

Enzyme Preparation. Histidinol dehydrogenase was purified from cells of *Salmonella typhimurium* strain *his01242* (*10*) or from an overexpression strain as described (*13*). The twice-crystallized enzyme appeared homogeneous on SDS−PAGE, and gave a specific activity of 12−17 units/mg (corresponding to k_{cat} of 9.2−13 s^{-1}). Before assay, a portion of the suspended crystals was dissolved in buffer containing 50 mM sodium glycine (pH 9.0) and 0.5 mM $MnCl_2$. This enzyme preparation was stable for at least 1 day. Enzyme concentration was determined spectrophotometrically (*26*) and is expressed as molarity of the 45 893 Da subunit (*27*).

Kinetic Measurements. Kinetic assays were conducted by continuously following the absorbance increase at 340 nm for the production of NADH or at 363 nm for the production of AcPAD (E = 9100 M^{-1} cm^{-1}). The standard assay mixture contained 50 mM sodium glycine (pH 9.0), 0.5 mM $MnCl_2$, 10 mM NAD, and 2 mM histidinol. Assay medium (1 mL) in a quartz cuvette was allowed to temperature equilibrate for 5 min in the 30 °C thermostated cuvette holder of a Perkin-Elmer 552A spectrophotometer. The assay was initiated by addition of enzyme. For deuterium KIE with histidinol as the variable substrate, protiated and various deuterated histidinols were present at 10−50 μM, and NAD or AcPAD was present at 10 mM (*21*). For K_M determinations with the alternative substrate imidazolyl propanediol, it was present at 100−500 μM, and NAD concentration was fixed at 20 mM. Deuterium KIE with NAD as the variable substrate was determined with 0.4−2.0 mM coenzyme, and 0.5 mM of protiated and various deuterated histidinols. With imidazolyl propanediol, the substrate was present at 2 mM, and the coenzyme concentrations varied from 1−5 mM.

Deuterium KIE at pH 6.7 were determined with buffer containing 50 mM sodium Hepes (pH 6.7) and 0.5 mM $MnCl_2$. Enzyme was prepared for assay as above. For K_M determinations with protiated and various deuterated histidinols, substrates were present at 10−50 μM, and NAD was present at 10 mM. For NAD kinetics, the coenzyme concentrations varied from 0.5 to 2 mM and protiated and various deuterated histidinols at 0.3 mM.

Steady-state kinetic measurements using (^{3}H,H)histidinol were done by following the absorbance at 340 nm as for normal kinetics and taking 100 μL samples at various times to measure the extent of [4(*R*)-^{3}H]NADH production. Samples were applied to columns of DEAE cellulose to separate histidinol, NAD, and NADH as described previously (*21*).

pH Profiles. For log(k_{cat}) and log(k_{cat}/K_M) pH profiles, enzyme crystals were dissolved in 50 mM sodium glycine (pH 9.0) and 0.5 mM $MnCl_2$. Enzyme solutions were added to assay buffer (1 mL) containing 50 mM glycine, 50 mM Hepes, 0.5 mM $MnCl_2$, and 10 mM NAD, previously titrated to desired pH values with NaOH and allowed to incubate at 30 °C for 5 min. Histidinol was added to start the reaction. For pH profiles with histidinol as the variable substrate, 10−100 μM histidinol was used, and NAD was present at 10 mM. For pH profiles with imidazolyl propanediol, the range of substrate used was 100−500 μM, with NAD present at 10 mM. With NAD as the variable substrate, the assay buffer contained 2 mM histidinol and 0.33−2 mM NAD. Results were analyzed by the program HA-BELL (*28*) and are reported with their standard errors.

Stopped-Flow Experiments. Rapid kinetic measurements were conducted with a Hi-Tech Scientific SF-61 Stopped-flow system. In the experiments described, production of NADH was monitored at 340 nm through an observation cell with a path length of 10 mm. Syringes were temperature equilibrated at 30 °C. An equal volume (55 μL) from each syringe was injected during each measurement. All buffers contained 50 mM sodium glycine (pH 9.0) and 0.5 mM $MnCl_2$. In multiple turnover experiments with histidinol, the enzyme syringe contained 182 μM subunit preincubated with 4 mM (H,H)histidinol or (D,D)histidinol, and the coenzyme syringe contained 20 or 10 mM NAD, respectively. In single turnover experiments the enzyme syringe contained 182 μM subunit preincubated with 98 μM (H,H)histidinol or 112 μM (D,D)histidinol, and the coenzyme syringe contained 10 mM NAD. In multiple turnover experiments with the alternative substrate imidazolyl propanediol, the enzyme syringe contained 9 μM subunit and 4 mM diprotiated or dideuterated imidazolyl propanediol and was mixed with a solution containing 20 mM NAD in the coenzyme syringe. Results reported were the means of at least four injections. Data from

Table 1: Isotope Effects for the Histidinol Dehydrogenase Reaction

	Histidinol		NAD		Histidinol with AcPAD	
substrate	^{D}V	$^{D}(V/K)$	^{D}V	$^{D}(V/K)$	^{D}V	$^{D}(V/K)$
(D,D)histidinol(pH 9.0)[a]	2.55 ± 0.13	1.30 ± 0.14	2.50 ± 0.2	1.94 ± 0.22	2.40 ± 0.30	2.40 ± 0.18
(D,H)histidinol(pH 9.0)	1.18 ± 0.08	1.13 ± 0.11	1.26 ± 0.09	1.22 ± 0.10	1.50 ± 0.14	1.77 ± 0.10
(H,D)histidinol(pH 9.0)	2.39 ± 0.22	1.19 ± 0.23	2.29 ± 0.13	1.46 ± 0.11	2.00 ± 0.09	1.26 ± 0.05
(D,D)histidinol(pH 6.7)	2.03 ± 0.21	2.14 ± 0.25	1.94 ± 0.17	1.52 ± 0.05	nd	nd
(D,H)histidinol(pH 6.7)	1.59 ± 0.13	1.38 ± 0.17	1.59 ± 0.21	1.38 ± 0.18	nd	nd
(H,D)histidinol(pH 6.7)	1.52 ± 0.12	1.32 ± 0.12	1.43 ± 0.19	1.29 ± 0.08	nd	nd

	imidazolyl propanediol		NAD	
substrate	^{D}V	$^{D}(V/K)$	^{D}V	$^{D}(V/K)$
(D,D)imidazolyl propanediol (pH 9.0)	2.40 ± 0.39	1.03 ± 0.23	2.59 ± 0.70	0.98 ± 0.21

[a] Preliminary KIE results with deuterated histidinols at pH 9.0 were reported in Grubmeyer (*34*). nd, not determined. With (D,D)histidinol, deuterides were transferred during both half-reactions. With (D,H) and (H,D)histidinols, deuterides were transferred during the first and second half-reactions, respectively.

multiple turnover experiments were fitted to the following equation (*29*):

$$[P]_{obs}/[E_o] = A_o(1 - e^{-k_1 t}) + k_{cat}t$$

where $[P]_{obs}/[E_o]$ is the stoichiometry of NADH produced per enzyme subunit, A_o is the burst stoichiometry extrapolated to zero time, k_1 is the rate for approach to equilibrium, k_{cat} is the steady-state for NADH production per enzyme subunit, and t is the time.

Isotope Partition. The isotope-trapping technique (*30*, *31*) was employed to determine the proportion of enzyme-bound histidinol that partitioned toward catalysis. A solution (50 μL) containing 50 mM sodium glycine (pH 9.0), 0.5 mM $MnCl_2$, and 95 μM enzyme subunit was preincubated with 80−230 μM [^{14}C]histidinol (specific activity 4×10^5 cpm/μmole) at 21 °C for 5 min, before injecting it into 450 μL of rapidly stirred "chase" solution containing 50 mM sodium glycine (pH 9.0), 0.5 mM $MnCl_2$, 11 mM histidinol, and 11 mM NAD, also at 21 °C. After 2 s, 100 μL of 30% perchloric acid was injected, and the sample was centrifuged to remove denatured enzyme. The supernatant was brought to pH 6.5 to 7.0 with KOH, chilled on ice, and then centrifuged to remove potassium perchlorate. The supernatant was then adjusted to 1 mL with 0.1 M sodium phosphate (pH 6.8) before separation. For the zero time sample, perchloric acid was added to the chase solution before the enzyme and labeled histidinol, and the sample was treated as described above. To determine the amount of [^{14}C]histidine produced from steady-state oxidation of [^{14}C]histidinol that was not initially enzyme bound, the [^{14}C]histidinol was added to the chase solution before enzyme and allowed to react for 2 s before addition of perchloric acid.

Separation of [^{14}C]histidine from [^{14}C]histidinol was performed according to Ciesla et al. (*32*). Samples were loaded onto a 1 mL column of Dowex 50X 4-400 cation-exchange resin preequilibrated with 1 M sodium acetate (pH 6.0), followed by 7 × 1 mL washes with 0.1 M sodium phosphate (pH 6.8) and then 4 × 1 mL washes with 6 M HCl. Fractions (1 mL) were collected, and a 200 μL aliquot of each was withdrawn for determination of radioactivity. [^{14}C]Histidine eluted in fractions 5, 6, and 7, and [^{14}C]-histidinol eluted in fractions 9 and 10. The proportion of enzyme-bound [^{14}C]histidinol trapped was calculated from the [^{14}C]histidine that appeared in the "trapped" sample, after correction for the steady-state production of [^{14}C]histidine and the reported stoichiometry and K_D of histidinol binding to the enzyme (*21*).

Kinetic Simulations. Kinetic simulations of HDH catalysis were conducted with the program KINSIM (*33*), modified to use with Macintosh computer by D. Wachsstock at Johns Hopkins University. In the simulation runs, default settings for flux and integral tolerances were used, which allowed the computer to determine the optimal time interval between each integration, such that the changes in substrate concentrations were within reasonable limits (*33*).

RESULTS

Isotope Effects with Histidinol. When (D,D)histidinol was used as the substrate for the HDH reaction at pH 9.0, a 2.55 ^{D}V isotope effect was observed (Table 1). The measured $^{D}V/K$ was 1.30. The results indicated a participation by one of the two hydride transfers in overall rate limitation. The availability of monodeuterated histidinol from HDH-catalyzed exchange reactions (*21*) made it possible to explore which step contributed to the isotope effects. The (H,D)histidinol [this compound was 65% (H,D) with the remainder unexchanged (D,D)histidinol] gave a 2.39 ^{D}V effect, with 1.19 $^{D}V/K$. When (D,H)histidinol [60% (D,H) with 40% (H,H)-histidinol] was employed as substrate, a ^{D}V effect of 1.18 was observed, $^{D}V/K$ was 1.13. The results thus demonstrate greater participation of the second (*pro-R*) hydride transfer step in ^{D}V, with lesser participation by the first (*pro-S*) hydride transfer.

Although the $^{D}V/K$ KIE observed with all deuterated substrates at pH 9.0 were small, use of enzymatically synthesized (^{3}H,H)histidinol gave rise to a readily measured 1.4-fold discrimination against tritium over the initial 5−10% conversion, confirming the detected $^{D}V/K$ effect in the first half-reaction.

When NAD was the varied substrate at pH 9.0, with (D,D)histidinol a $^{D}V/K$ of 1.94 was observed. The use of (D,H)histidinol gave rise to a $^{D}V/K$ of 1.22, and (H,D)-histidinol showed a $^{D}V/K$ of 1.46.

At pH 6.7, (D,D)histidinol showed a ^{D}V effect of 2.03, and $^{D}V/K$ of 2.14. With (D,H)histidinol, ^{D}V measured was 1.59, and $^{D}V/K$ was 1.38. The ^{D}V effect with (H,D)histidinol was 1.52, and $^{D}V/K$ was 1.32.

Contamination of the monodeuterated histidinols could skew the values of ^{D}V if the enzyme discriminates against

Table 2: pK_a Values for Histidinol Dehydrogenase

substrate	pK_a	
	k_{cat}	k_{cat}/K_M
histidinol	8.17 ± 0.06	8.35 ± 0.08
NAD	7.92 ± 0.02	7.92 ± 0.02
imidazolyl propanediol	7.76 ± 0.05	7.72 ± 0.07

deuterated histidinol molecules (i.e., if there is a $^{D}V/K$ effect). The mechanism of HDH, with a tightly bound aldehyde-level intermediate, is such that discrimination occurs in the first half-reaction. To determine the severity of this problem, we measured the ^{D}V effects in synthetically constructed mixtures of (H,H) and (D,D)histidinols at pH 9.0 and pH 6.7 (data not shown). At pH 9.0, where $^{D}V/K$ effects are slight (Table 1), the measured ^{D}V was a linear function of the amount of (H,H)histidinol present in mixtures with (D,D)-histidinol. Thus, the ^{D}V KIEs measured with deuterated histidinols at pH 9.0 are largely unaffected by discrimination against contaminants. However, at pH 6.7, the magnitude of ^{D}V was a nonlinear function of the proportion of (H,H)-histidinol, in keeping with the substantial value of $^{D}V/K$ (2.14; Table 1). Using the data from the synthetic mixtures, we calculated that, for the contaminated deuterated histidinols, a true ^{D}V value of 2.0 for (D,H)histidinol at pH 6.7 would be reduced to an observed value of 1.6 by discrimination in favor of the 40% contaminating (H,H)histidinol, whereas a ^{D}V effect of 1.25 for (H,D)histidinol would be inflated to 1.5 by the 35% contaminating (D,D)histidinol. Thus, at pH 6.7, the measured values of ^{D}V with deuterated histidinols underestimate the extent to which the first hydride transfer has now become more rate limiting.

Isotope Effects with Alternative Substrates. Adams (*2*) reported that the k_{cat} of HDH with AcPAD was 36% of that with NAD. With AcPAD as the cofactor, (D,D)histidinol isotope effects were similar to those with NAD, with ^{D}V of 2.4 and $^{D}V/K$ of 2.4. However, the monodeuterated histidinols gave different results with this alternative cofactor. For (D,H)histidinol, ^{D}V was 1.5, with $^{D}V/K$ of 1.77, and with (H,D)histidinol, ^{D}V was 2.0 and $^{D}V/K$ was 1.26.

The alternative substrate imidazolyl propanediol is utilized with k_{cat} 140-fold lower than histidinol, and k_{cat}/K_M was 2000-fold less than histidinol (*5*). With this alternative substrate, a ^{D}V of 2.4 and a $^{D}V/K$ of 1.03 were measured. With NAD as the variable substrate, a $^{D}V/K$ of 0.98 was measured. Attempts to synthesize monodeuterated imidazolyl propanediols were frustrated by the inability of the alternative substrate to support either imidazolyl propanediol/NADH or NAD/NADH exchange reactions (unpublished observations).

The use of 96% D_2O in the assay medium gave a ^{D_2O}V isotope effect of 1.9. Proton inventories were slightly convex down (not shown), suggesting involvement of more than a single proton in the overall effect (*35*).

pH Studies. The log(k_{cat}) and log(k_{cat}/K_M) titration profiles for the overall reaction with histidinol as the variable substrate indicated that the deprotonated form of a single ionizable group with pK_a of 8.17 and 8.35, respectively, was essential for catalysis (Table 2). Both log(k_{cat}) and log(k_{cat}/K_M) pH profiles with NAD as the variable substrate were similar with pK_a values of 7.92. The log(k_{cat}) and log(k_{cat}/K_M) titration curves with imidazolyl propanediol as the variable substrate showed a single essential base with pK_a values of 7.76 and 7.72, respectively.

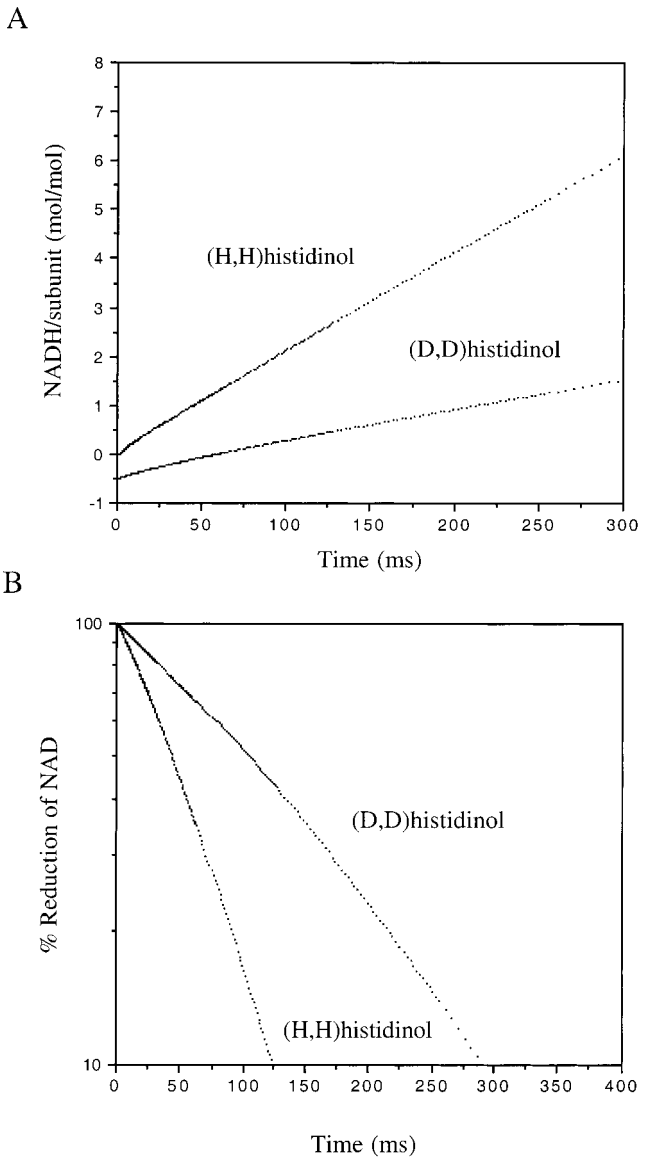

FIGURE 1: Stopped-flow studies with HDH. Panel A shows NADH production with (H,H) and (D,D)histidinol from multiple turnover experiments. NADH production with (D,D)histidinol has been offset to allow comparison. Panel B shows first-order plots of percent NAD reduction against time with (H,H) and (D,D)histidinol from single turnover experiments.

Stopped-Flow Studies. In multiple turnover stopped-flow experiments with (H,H)histidinol, the formation of NADH was slightly biphasic, with an initial phase with stoichiometry of 0.12 mol of NADH·mol of subunit^{-1} whose rate for approach to equilibrium was 40 s^{-1}, followed by a steady-state phase of 17 mol of NADH·mol of subunit^{-1} (corresponding to a k_{cat} of 8.5 s^{-1}; Figure 1A). Multiple turnover experiments with (D,D)histidinol showed that the biphasic appearance was enhanced, with a burst stoichiometry of 0.25 mol of NADH·mol of subunit^{-1}, a rate for approach to equilibrium of 15 s^{-1}, and a steady-state turnover rate of 5.7 mol of NADH·mol of subunit^{-1} (corresponding to a k_{cat} of 2.9 s^{-1}). In multiple turnover experiments with diprotiated and dideuterated imidazolyl propanediols, the initial rates of NADH production were linear, at 0.17 mol of NADH·mol of subunit^{-1} (corresponding to a k_{cat} of 0.085 s^{-1}) and

Scheme 1. Kinetic Scheme for HDH[a]

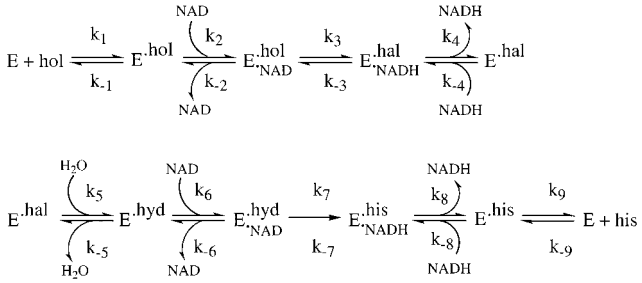

[a] E, HDH; hol, histidinol; hal, histidinal; hyd, hydrated histidinal; his, histidine. In this scheme, the oxidation of histidinal is via an aldehyde hydrate intermediate,

0.06 mol of NADH·mol of subunit^{-1} (corresponding to a k_{cat} of 0.03 s^{-1}), respectively, and no rapid phase was observed in either case (not shown). We have repeated the experiments at different enzyme concentrations [with both (H,H) and (D,D)histidinols] and observed similar NADH burst stoichiometries, rates for approach to equilibrium, and steady-state turnover rates.

To rule out the possibility that a very rapid stoichiometric burst of NADH production had been overlooked, single turnover experiments with a molar excess of enzyme subunit over histidinol were also performed (Figure 1B). With (H,H)- and (D,D)histidinol, first order plots of the reduction of NAD were basically linear. NADH was formed in 2:1 stoichiometry with the histidinol present, showing that no rapid phase of NADH production had been missed.

Isotope Partitioning with Histidinol. Isotope trapping of enzyme·[^{14}C]histidinol binary complexes by NAD showed that 50−75% of the bound histidinol was trapped as [^{14}C]-histidine.

Simulations of HDH Catalysis. On the basis of previous kinetic data (*5*, *19*−*21*) and the results presented here, a kinetic mechanism for HDH catalysis at pH 9 can be constructed using Scheme 1 and the resultant behavior simulated with KINSIM (*33*). During the simulations, the on- and off-rates for histidine were varied to maintain the reported K_D value of 1 mM (*5*), and the on- and off-rates for NAD and NADH were varied to maintain their reported K_D values of 0.8 and 0.3 mM, respectively (*20*). Kinetic simulations using the kinetic constants shown in Table 3 for (H,H)histidinol showed a biphasic pattern, with a burst size of 0.1 mol of NADH·mol of subunit^{-1}, followed by a steady-state rate of 11 s^{-1} (Figure 2A). Employing intrinsic deuterium isotope effects of 5 for each hydride transfer step, simulation for reaction with (D,D)histidinol showed a burst size of 0.25 NADH·mol of subunit^{-1}, and a ^{D}V KIE of 2.50. Simulations for (D,H) and (H,D)histidinols yielded ^{D}V KIEs of 1.29 and 2.20, respectively (data not shown), which are close to the experimentally determined values. Simulated plots of NAD reduction against time in single turnover experiments with (H,H)- and (D,D)histidinols showed similar rates and patterns as the actual experimental data (Figure 2B).

Table 3: Kinetic Constants Used for Simulations[a]

constant	value	source
k_1	1×10^6 M^{-1} s^{-1}	k_{cat}/K_M for histidinol
k_{-1}	10 s^{-1}	K_D and k_1 for histidinol (*21*)
k_2	0.03×10^6 M^{-1} s^{-1}	$3 \times k_{cat}/K_M$ for NAD in overall reaction
k_{-2}	24 s^{-1}	K_D and k_2 for NAD (*20*)
k_3[b]	160 s^{-1}	rapid and reversible first hydride transfer (see text)
k_{-3}[b]	640 s^{-1}	rapid and reversible first hydride transfer (see text)
k_4[b]	150 s^{-1}	rapid product release (see text)
k_{-4}	0.5×10^6 M^{-1} s^{-1}	k_4 and K_I for NADH (*20*)
k_5[b]	500 s^{-1}	rapid and poorly reversible formation of histidinal adduct (see text)
k_{-5}[b]	10 s^{-1}	rapid and poorly reversible formation of histidinal adduct (see text)
k_6	0.03×10^6 M^{-1} s^{-1}	as k_2
k_{-6}	24 s^{-1}	as k_{-2}
k_7	40 s^{-1}	irreversible second hydride transfer (see text)
k_{-7}	0 s^{-1}	irreversible second hydride transfer (see text)
k_8	150 s^{-1}	as k_4
k_{-8}	0.5×10^6 M^{-1} s^{-1}	as k_{-4}
k_9	1000 s^{-1}	rapid release of histidine (see text)
k_{-9}	1×10^6 M^{-1} s^{-1}	k_9 and K_I for histidine (*5*)

[a] Kinetic constants are based in Scheme 1. Default settings for integral and flux tolerances were used in the simulations. [b] This value was adjusted to give optimal behavior in the simulation.

DISCUSSION

The results presented in this paper allow several important conclusions to be drawn about the kinetic mechanism of *Salmonella* HDH. The overall reaction consists of two partial reactions, oxidation of the alcohol substrate and the tightly bound aldehyde intermediate (*1*−*3*, *7*, *8*, *36*). In previous work (*21*), we found that an NAD/NADH exchange arising solely from the first half-reaction proceeded at 3-fold higher rate than overall catalysis, suggesting that the first half-reaction does not provide a clear rate-limiting step.

At pH 9.0, a 2.5-fold ^{D}V isotope effect was observed with dideuterated histidinol, indicating that one of the two hydride transfers participates in rate limitation. With monodeuterated histidinols, we were able to determine that the second hydride transfer accounted for nearly all the observed ^{D}V isotope effects, with only modest participation by the first hydride transfer. The only alternative interpretation for these data is that the ^{D}V isotope effect is actually an α-secondary isotope effect arising from bond-reordering events occurring after the first hydride transfer from histidinol and before the second hydride transfer, such as the hydration of histidinal. The observed KIE is far greater than previously observed α-secondary effects [between 1.22 and 1.34 for dehydrogenases (*37*)], including those for aldehyde hydration [1.4 (*38*)], leading us to reject this hypothesis.

Product inhibition, binding, and isotope-exchange experiments have firmly established that at pH 9.0 the first half-reaction of HDH is ordered, with histidinol binding preceding coenzyme (*7*, *8*, *20*, *21*). The small magnitude of the $^{D}V/K$ effects for deuterated histidinols, together with histidinol isotope-trapping experiments reported here, support this conclusion. Nevertheless, the $^{D}V/K$ effect with (D,D)-histidinol was not unity, indicating a random component to the kinetic pathway (*39*). Since the aldehyde-level intermediate does not dissociate from the active site over catalytic time scales (*1*, *2*, *7*, *8*), the expressed $^{D}V/K$ of 1.3 with (D,D)-histidinol, confirmed by the 1.4-fold $^{T}V/K$ effect with (^{3}H,H)-histidinol reported here, could only arise from the first half-reaction. Results with isotope-trapping experiments also showed that 75% of the preformed enzyme·histidinol binary complex could be trapped by NAD. These findings indicate

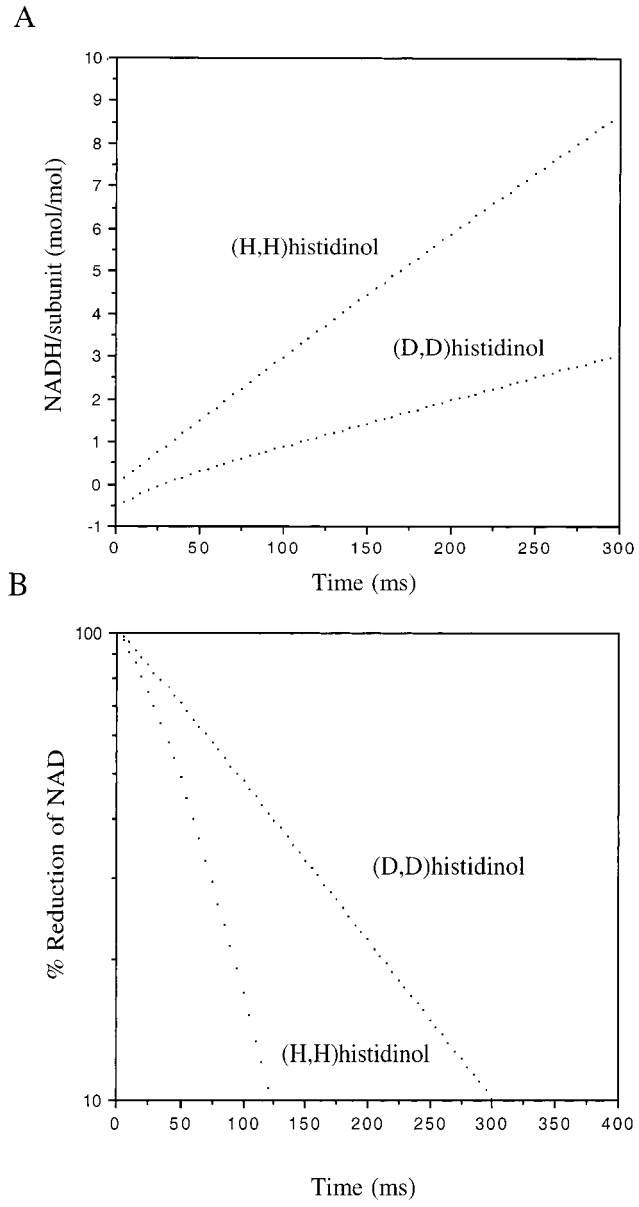

FIGURE 2: Simulations of reaction time-courses based on Scheme 1 and kinetic constants from Table 3. Panel A shows NADH production with (H,H) and (D,D)histidinol under multiple turnover conditions. NADH production with (D,D)histidinol has been offset to allow comparison. Panel B shows first-order plots of NAD reduction against time with (H,H) and (D,D)histidinol under single turnover conditions.

a minor route for histidinol dissociation from the enzyme·histidinol·NAD ternary complex.

On the basis of the studies reported here and by Grubmeyer et al. (*5*), which indicated a relatively rapid first half-reaction and a more rate-limiting second half-reaction for HDH, we expected burst-type kinetics with stoichiometric formation of NADH. Surprisingly, stopped-flow results with (H,H)- and (D,D)histidinol did not show a stoichiometric pre-steady-state burst of NADH production under multiple turnover conditions. Instead, the enzyme showed an initial rapid phase with a stoichiometry of 0.12 mol of NADH·mol of subunit^{-1} with (H,H)histidinol, which increased to 0.25 mol of NADH·mol of subunit^{-1} when (D,D)histidinol was employed. In a variety of control experiments not reported here, we confirmed that, as isolated, HDH did not contain bound coenzyme (see also ref *36*), nor was the enzyme in a "reduced" or "oxidized" state that would allow for an initial reduction of NAD in the absence of histidinol or oxidation of histidinol in the absence of NAD, respectively. As single turnover experiments showed that no burst of NADH production faster than the resolving capability of the apparatus had occurred, the reaction events within the first half-reaction probably also participate in the overall rate limitation.

Alternative substrates and catalysis at suboptimal pH were employed to determine the extent of rate limitation by the first half-reaction. Experiments with AcPAD showed that the overall ^{D}V for (D,D)histidinol was only slightly changed (Table 1). However, the ^{D}V effects with (D,H)histidinol was increased from 1.26 with NAD to 1.50 with AcPAD, whereas the ^{D}V effects with (H,D)histidinol decreased from 2.29 with NAD to 2.00 with this alternative coenzyme, indicating a shift in rate limitation from the second to the first hydride transfer. As the first hydride transfer becomes more rate-limiting with this alternative coenzyme, the contamination in the monodeuterated histidinol preparations skewed the magnitude of the ^{D}V effects, lessening both the increase in ^{D}V for (D,H)histidinol and the decrease in ^{D}V for (H,D)-histidinol.

When the HDH reaction was conducted at pH 6.7, which results in an approximate 20-fold decrease in k_{cat}, the ^{D}V isotope effect for (D,D)histidinol decreased from 2.55 to 2.03. The $^{D}V/K$ effect rose from 1.3 to 2.14, and the pattern of KIE with monodeuterated histidinols was different when compared to the KIEs at pH 9.0. The decreased ^{D}V effect at lower pH (2.39−1.32) for (H,D)histidinol and the increased ^{D}V effect (1.26−1.59) for (D,H)histidinol suggested that the first half-reaction had become more rate limiting at pH 6.7. The KIE results with AcPAD and at pH 6.7 again indicated that the rates for the two half-reaction sequences did not differ significantly, in support of the conclusion from stopped-flow studies, which suggested partial rate limitation for both hydride transfers. Recent steady-state studies with *Brassica* HDH using synthetic histidinal at pH 7.2 showed that oxidation of histidinal to histidine occurred at about 3-fold faster than overall catalysis (*8*). Experiments with this synthetic substrate are difficult to interpret, given the known lability of the compound (*7*, *40*) and the reactivity of aldehydes with amine-containing buffers (*41*).

KIE study with the alternative substrate imidazolyl propanediol showed that the hydride transfer was at least partially rate limiting (Table 1). Stopped-flow studies with both (H,H)- and (D,D)imidazolyl propanediol showed linear initial rates of NADH production identical to the steady-state rates, indicating that the first hydride transfer with this alternative substrate was rate limiting. The unity $^{D}V/K$ isotope effects with imidazolyl propanediol and NAD suggested high commitment to catalysis for the enzyme·imidazolyl propanediol·NAD ternary complex. The inability of imidazolyl propanediol to support imidazolyl propanediol/NADH or NAD/NADH isotope exchange supports the formation of such a tightly associated ternary complex.

We attempted to simulate the HDH reaction at pH 9.0 using KINSIM (*33*), with kinetic constants estimated here and in earlier work. The key assumptions in our model, shown in Scheme 1 and Table 3, are (1) attack of nucleophile on histidinal is rapid and favorable, (2) NADH release rates for both half-reactions are identical and rapid, (3) as discussed above, *overall* rates of the first and second half-

reactions are not dramatically different, allowing both to contribute to overall rate limitation, (4) the oxidation of histidinol to histidinal is rapid, with an internal K_{eq} less than 1, and (5) intrinsic deuterium isotope effects for both hydride transfers are identical. These assumptions have not explicitly been tested, although they are not unexpected. An internal K_{eq} of 0.25 for the oxidation of histidinol to histidinal used in the simulation is within the range of K_{eq} values reported for alcohol oxidations. Studies with horse liver ADH using benzyl alcohol demonstrated an unfavorable internal equilibrium toward benzaldehyde formation (*42*, *43*). The intrinsic isotope effect (^{D}k) of 5 used in the simulation is within the ^{D}k for the oxidation of cyclohexanol and 2-propanol by ADH (*44*, *45*) and greater than the ^{D}k of about 3 reported for the oxidation of benzaldehyde by yeast aldehyde dehydrogenase (*46*). Other ^{D}k values tested in the simulations did not yield the experimentally determined ^{D}V isotope effects when modeled for monodeuterated histidinol. A slower on-rate for the first NAD molecule (k_2) resulted in a lag phase before NADH production, although varying the on-rate for histidinol (k_1) by 2-fold had minimal effect on the simulated profiles. When the rate of hydride transfer from histidinol (k_3) was less than 3-fold higher than the rate of hydride transfer from histidinal (k_7), the simulations did not show a pre-steady-state NADH burst, and above a 6-fold difference between the two hydride transfer rates the pre-steady-state NADH burst was larger than the values obtained. Finally, increasing both NADH release rates (k_{-4} and k_{-8}) by 2-fold resulted in a ^{D}V effect above 1.26 when simulated for (D,H), whereas decreasing both NADH release rates by 2-fold resulted in a ^{D}V effect below 2.20 when simulated for (H,D)histidinols. The simulated mechanism, although not a unique solution, provides reasonable fits to the stopped-flow data.

An active-site base residue is required to catalyze proton transfers in overall catalysis. Our results with log(k_{cat}) and log(k_{cat}/K_M) versus pH profiles showed that a single ionizable group with a pK_a ranging 7.7−8.4 was responsible for the formation of productive complex and catalysis (Table 2). A possible candidate for the enzymic base is the α-amino group of histidinol, for which we determined a solution pK_a of 8.75, identical to that of alaninol (results not shown). To address whether the α-amino group of histidinol was being titrated, we examined the pH dependence of catalysis with the alternative substrate imidazolyl propanediol. The similarity of pK_a values of the base residue to that with histidinol indicated that the observed pK_a value comes from an enzymic base. Investigation of the nature of the enzymic base is reported in the following paper in this issue.

ACKNOWLEDGMENT

We thank Dr. John S. Blanchard for the use of the stopped-flow apparatus and Dr. Peter A. Tipton for providing assistance in acquiring KINSIM.

REFERENCES

1. Adams, E. (1954) *J. Biol. Chem. 209*, 829−846.
2. Adams, E. (1955) *J. Biol. Chem. 217*, 325−344.
3. Feingold, D. S., and Franzen, J. S. (1981) *Trends Biochem. Sci. 6*, 103−105.
4. Davies, D. D., Teixeria, A., and Kenworthy, P. (1972) *Biochem. J. 127*, 335−343.
5. Grubmeyer, C. T., Insinga, I., Bhatia, M., and Moazami, N. (1989) *Biochemistry 28*, 8174−8180.
6. Nagai, A., Shimoinishiyama, H., Ohta, D., Scheidegger, A., Esaki, N., and Soda, K. (1995) *Biosci. Biotech. Biochem. 59*, 1370−1371.
7. Görisch, H., and Hölke, W. (1985) *Eur. J. Biochem. 150*, 305−308.
8. Kheirolomoom, A., Mano, J.-i., Nagai, A., Ogawa, A., Iwasaki, G., and Ohta, D. (1994) *Arch. Biochem. Biophys. 312*, 493−500.
9. Eccleston, E. D., Thayer, M. L., and Kirkwood, S. (1979) *J. Biol. Chem. 254*, 11399−11404.
10. Grubmeyer, C. T., and Gray, W. R. (1986) *Biochemistry 25*, 4778−4784.
11. Grubmeyer, C. T., and Insinga, S. (1990) *J. Am. Chem. Soc. 112*, 5906−5908.
12. Nagai, A., Kheirolomoom, A., and Ohta, D. (1993) *J. Biochem. 114*, 856−861.
13. Teng, H., Segura, E., and Grubmeyer, C. (1993) *J. Biol. Chem. 268*, 14182−14188.
14. Warren, W. A. (1970) *J. Biol. Chem. 245*, 1675−1681.
15. Corbier, C., Seta, F. D., and Branlant, G. (1992) *Biochemistry 31*, 12532−12535.
16. Eisses, K. Th. (1989) *Bioorg. Chem. 17*, 268−274.
17. Oppenheimer, N. J., and Handlon, A. L. (1992) In *The Enzymes* (Sigman, D. S., Ed.) 3rd ed.; Vol. 20, pp 453−505, Academic Press, San Diego.
18. Olson, L. P., Luo, J., Almarsson, Ö., and Bruice, T. C. (1996) *Biochemistry 35*, 9782−9791.
19. Görisch, H. (1979) *Biochem. J. 181*, 153−157.
20. Bürger, E., and Görisch, H. (1981) *Eur. J. Biochem. 116*, 137−142.
21. Grubmeyer, C. T., Chu, K.-W., and Insinga, S. (1987) *Biochemistry 26*, 3369−3373.
22. Ordman, A. B., and Kirkwood, S. (1977) *Biochim. Biophys. Acta 481*, 25−32.
23. Campbell, R. E., Sala, R. F., van de Rijn, I., and Tanner, M. E. (1997) *J. Biol. Chem. 272*, 3416−3422.
24. Bradbury, S. L., and Jakoby, W. B. (1971) *J. Biol. Chem. 246*, 1834−1840.
25. Heute-Pérez, J. A., Wu, J. C., Whitby, F. G., and Wang, C. C. (1995) *Biochemistry 34*, 13889−13894.
26. Loper, J. C. (1968) *J. Biol. Chem. 243*, 3264−3272.
27. Carlomagno, M. S., Chiariotti, L., Alifano, P., Nappo, A. G., and Bruni, C. B. (1988) *J. Mol. Biol. 203*, 585−606.
28. Cleland, W. W. (1979) *Methods Enzymol. 63*, 103−138.
29. Johnson, K. A. (1992) In *The Enzymes* (Sigman, D. S., Ed.) 3rd ed.; Vol. 20, pp 1−61, Academic Press, San Diego.
30. Rose, I. A. (1980) *Methods Enzymol. 64*, 47−59.
31. Rose, I. A. (1995) *Methods Enzymol. 249*, 315−340.
32. Ciesla, Z., Salvatore, F., Broach, J. R., Artz, S. W., and Ames, B. N. (1975) *Anal. Biochem. 63*, 44−55.
33. Barshop, B. A., Wrenn, R. F., and Frieden, C. (1983) *Anal. Biochem. 130*, 134−145.
34. Grubmeyer (1991) in *Enzymology and Molecular Biology of Carbonyl Metabolism 3* (Weiner, H., Wermuth, B., and Crabb, D. W., Eds.) pp 105−112, Plenum Press, New York.
35. Schowen, K. B., and Schowen, R. L. (1982) *Methods Enzymol. 87*, 551−606.
36. Loper, J. C., and Adams, E. (1965) *J. Biol. Chem. 240*, 788−795.
37. Cook, P. F., Oppenheimer, N. J., and Cleland, W. W. (1981) *Biochemistry 20*, 1817−1825.
38. Lewis, C. A., Jr., and Wolfenden, R. (1977) *Biochemistry 22*, 4886−4895.
39. Cook, P. F., and Bertagnolli, B. L. (1987) in *Pyridine Nucleotide Coenzymes Part A* (Dolphin, D., Avramovic, O., and Poulsen, R., Eds.) pp 405−447, John Wiley, New York.
40. Adams, E. (1955) *J. Biol. Chem. 217*, 317−324.
41. Henehan, G. T. M., Chang, S. H., and Oppenheimer, N. J. (1995) *Biochemistry 34*, 12294−12301.

42. Anderson, D. C., and Dahlquist, F. W. (1982) *Arch. Biochem. Biophys. 217*, 226−235.
43. Shearer, G. L., Kim, K., Lee, K. M., Wang, C., K., and Plapp, B. V. (1993) *Biochemistry 32*, 11186−11194.
44. Cook, P. F., and Cleland, W. W. (1981) *Biochemistry 20*, 1791−1805.
45. Cook, P. F., and Cleland, W. W. (1981) *Biochemistry 20*, 1805−1816.
46. Scharschmidt, M., Fisher, M. A., and Cleland, W. W. (1984) *Biochemistry 23*, 5471−5478.

BI982757X